Supplementary Material

Table S1. Digitized landmarks shown in Fig. 3, where the white dashed line indicates the midsagittal axis used to locate several landmarks. The sampled *A. l. insularis* retain their peg-like P3 or its alveolus, enabling landmark placement.

Dorsal landmarks:

1. Rostral-most of internasal suture
2. Intersection between frontonasal suture and midsagittal plane
3. Interparietal-occipital suture on midsagittal plane
4. Caudal-most of occipital on midsagittal plane
5. Intersection between parietal/interparietal, occipital, and temporal bones (asterion)
6. Lateral–most of occipital-temporal suture
7. Caudal-most of squamosal root of zygomatic arch
8. Rostral-most of squamosal root of zygomatic arch
9. Caudal root of postorbital process
10. Lateral edge of zygomatic arch directly lateral to landmark 9 (lateral surface)
11. Narrowest point of the frontal (postorbital constriction)
12. Lateral edge of zygomatic arch directly lateral to landmark 11 (lateral surface)
13. Caudal-most of frontomaxillary suture
14. Intersection between frontal, maxillary, and premaxillary bones
15. Rostral-most of maxillary-premaxillary suture
16. Caudal-most of nasopremaxillary suture
17. Rostral-most of nasopremaxillary suture

Ventral landmarks:

1. Rostral-most of internasal suture
2. Midpoint between rostral incisor edges
3. Rostral-most of incisive foramen on midsagittal plane
4. Caudal-most of incisive foramen on midsagittal plane
5. Intersection between palatine-maxillary suture and midsagittal plane
6. Caudal-most of palatine bone on midsagittal plane (posterior nasal spine)
7. Intersection between basisphenoid-basioccipital suture and midsagittal plane
8. Rostral-most of foramen magnum on midsagittal plane
9. Caudal-most of foramen magnum on midsagittal plane
10. Lateral-most of foramen magnum
11. Lateral base of occipital condyle
12. Caudal-most of auditory bulla at junction with lateral edge of paroccipital process
13. Caudal-most of external auditory meatus
14. Rostral-most of external auditory meatus
15. Lateral edge of overlap between external auditory meatus and squamosal
16. Caudal edge of zygomaticotemporal suture
17. Caudal extremity of anterior edge of the zygomatic arch squamosal root
18. Rostral edge of zygomaticotemporal suture
19. Lateral edge of zygomatic arch directly lateral to landmark 6 (lateral surface)
20. Lateral edge of zygomatic arch directly lateral to landmark 34 (lateral surface)

21. Caudal edge of zygomaxillary suture
22. Midrostral extremity of posterior edge maxillary root of the zygomatic arch
23. Rostral edge of zygomaxillary suture
24. Lateral edge of rostrum directly lateral to landmark 29
25. Lateral-most of premaxillary-maxillary suture
26. Lateral-most of incisor
27. Lateral edge of nasal
28. Medial-most of premaxillary-maxillary suture
29. Medial base of masseteric tubercle
30. Rostral-most of alveolus of P3
31. Midpoint between lingual edges of the alveoli of P3 and P4
32. Midpoint between lingual edges of P4 and M1 on alveolus
33. Midpoint between lingual edges of M1 and M2 on alveolus
34. Midpoint between lingual edges of M2 and M3 on alveolus
35. Caudal-most of M3 on alveolus
36. Rostromedial edge of posterior maxillary notch
37. Lateral-most of parapterygoid-alisphenoid suture
38. Point on rostral edge of auditory bulla intersecting a line connecting landmarks 17 and 40
39. Mid-caudal edge of foramen ovale at intersection with rostral edge of auditory bulla
40. Lateral-most of basisphenoid-basioccipital suture (intersecting auditory bulla)
41. Point on medial edge of auditory bulla directly medial to landmark 13

Table S2. ANOVA results for eight linear models: (a) four centroid size models comparing the two most sampled subspecies within each species (both views) and (b) four Procrustes shape coordinate models comparing the two most sampled subspecies within each species (both views), all using subspecies as the sole predictor.

	Dorsal view			Ventral view		
	R^2	Z	p	R^2	Z	p
a. Centroid size (log)						
A. h. harrisii — A. h. saxicolus	0.076	1.160	0.135	0.004	-0.613	0.729
A. l. insularis — A. l. leucurus	0.210	2.657	**0.002**	0.071	1.387	0.086
b. Procrustes shape						
A. h. harrisii — A. h. saxicolus	0.027	-0.088	0.540	0.030	-0.126	0.548
A. l. insularis — A. l. leucurus	0.177	5.268	**0.001**	0.178	4.817	**0.001**

Notes: R^2=R-squared values; Z=effect sizes (standard deviates of F sampling distributions); p=p-values based on 999 permutations. RRPP was used to evaluate the fit of each linear model using sequential sums of squares. Ordinary least squares (OLS) were used to estimate model coefficients. Significant model terms ($p<0.05$) are in bold. These models omit specimens damaged in either view (from the respective view).

Table S3.

	Predicted (frequencies)							
Actual	*A. harrisii harrisii*	*A. harrisii saxicolus*	*A. interpres*	*A. leucurus cinnamomeus*	*A. leucurus insularis*	*A. leucurus leucurus*	*A. nelsoni*	Total
A. harrisii harrisii	10	4	6	1	0	4	0	25
A. harrisii saxicolus	6	0	1	0	0	1	0	8
A. interpres	2	1	29	0	0	1	1	34
A. leucurus cinnamomeus	2	0	0	0	0	1	0	3
A. leucurus insularis	0	0	0	0	9	0	0	9
A. leucurus leucurus	4	0	2	0	0	20	6	32
A. nelsoni	1	1	2	0	0	4	30	38

	Predicted (percentages)							
Actual	*A. harrisii harrisii*	*A. harrisii saxicolus*	*A. interpres*	*A. leucurus cinnamomeus*	*A. leucurus insularis*	*A. leucurus leucurus*	*A. nelsoni*	Total
A. harrisii harrisii	40%	16%	24%	4%	0%	16%	0%	100%
A. harrisii saxicolus	75%	0%	13%	0%	0%	13%	0%	100%
A. interpres	6%	3%	85%	0%	0%	3%	3%	100%
A. leucurus cinnamomeus	67%	0%	0%	0%	0%	33%	0%	100%
A. leucurus insularis	0%	0%	0%	0%	100%	0%	0%	100%
A. leucurus leucurus	13%	0%	6%	0%	0%	63%	19%	100%
A. nelsoni	3%	3%	5%	0%	0%	11%	79%	100%

Total correctly classified
98
All classifications
149
Overall classification accuracy
66%

Table S4. Climate PCA loadings showing contributions of 19 climatic variables to each PC axis.

	Description	PC1	PC2
BIO1	Annual Mean Temperature	-0.34	0.04
BIO2	Mean Diurnal Range (Mean of monthly (max temp - min temp))	-0.06	-0.02
BIO3	Isothermality (BIO2/BIO7) (×100)	-0.17	0.29
BIO4	Temperature Seasonality (standard deviation ×100)	0.14	-0.37
BIO5	Max Temperature of Warmest Month	-0.28	-0.14
BIO6	Min Temperature of Coldest Month	-0.32	0.15
BIO7	Temperature Annual Range (BIO5-BIO6)	0.08	-0.31
BIO8	Mean Temperature of Wettest Quarter	-0.12	0.14
BIO9	Mean Temperature of Driest Quarter	-0.29	-0.05
BIO10	Mean Temperature of Warmest Quarter	-0.31	-0.11
BIO11	Mean Temperature of Coldest Quarter	-0.34	0.14
BIO12	Annual Precipitation	0.24	0.28
BIO13	Precipitation of Wettest Month	0.13	0.39
BIO14	Precipitation of Driest Month	0.31	0.00
BIO15	Precipitation Seasonality (Coefficient of Variation)	-0.14	0.36
BIO16	Precipitation of Wettest Quarter	0.17	0.37
BIO17	Precipitation of Driest Quarter	0.31	-0.01
BIO18	Precipitation of Warmest Quarter	0.09	0.30
BIO19	Precipitation of Coldest Quarter	0.12	0.07

Notes: PCA utilized 19 standardized bioclimatic variables from WorldClim (version 2; Fick and Hijmans 2017). Variables were centered and scaled before analysis to address measurement unit differences. Variable descriptions were obtained from https://www.worldclim.org/bioclim. Fig. 8 displays these PC1–2 as scatterplots with explained variance.

Table S5. 2B-PLS analysis of climate variable covariation with (a) centroid sizes and (b) Procrustes coordinates across within each species.

	Dorsal view			Ventral view		
	r-PLS	p	Z	r-PLS	p	Z
a. Centroid size (log)						
A. harrisii	0,496	**0,021**	1,997	0,518	**0,013**	2,189
A. interpres	0,525	**0,008**	2,361	0,576	**0,002**	2,641
A. leucurus	0,536	**0,001**	3,079	0,392	**0,024**	1,924
A. nelsoni	0,332	0,137	1,138	0,238	0,379	0,296
b. Procrustes shape						
A. harrisii	0,589	0,326	0,435	0,670	0,136	1,155
A. interpres	0,698	0,120	1,162	0,687	0,132	1,162
A. leucurus	0,773	**0,001**	4,265	0,802	**0,001**	3,329
A. nelsoni	0,555	0,314	0,517	0,519	0,594	-0,243

Notes: r-PLS=correlation coefficient among scores of projected values on the first singular vectors of the Procrustes shape variables block (or logged centroid size block) and the climatic variables block; p=p-values based on 999 iterations of random permutations (significant associations, $p<0.05$, are in bold); Z=multivariate effect size. The climatic variables block is based on 19 bioclimatic variables of each sampled locality downloaded from and described in WorldClim (version 2) (Fick and Hijmans 2017; https://www.worldclim.org/). The climatic variables were standardized by centering and scaling the data to account for their having different units.

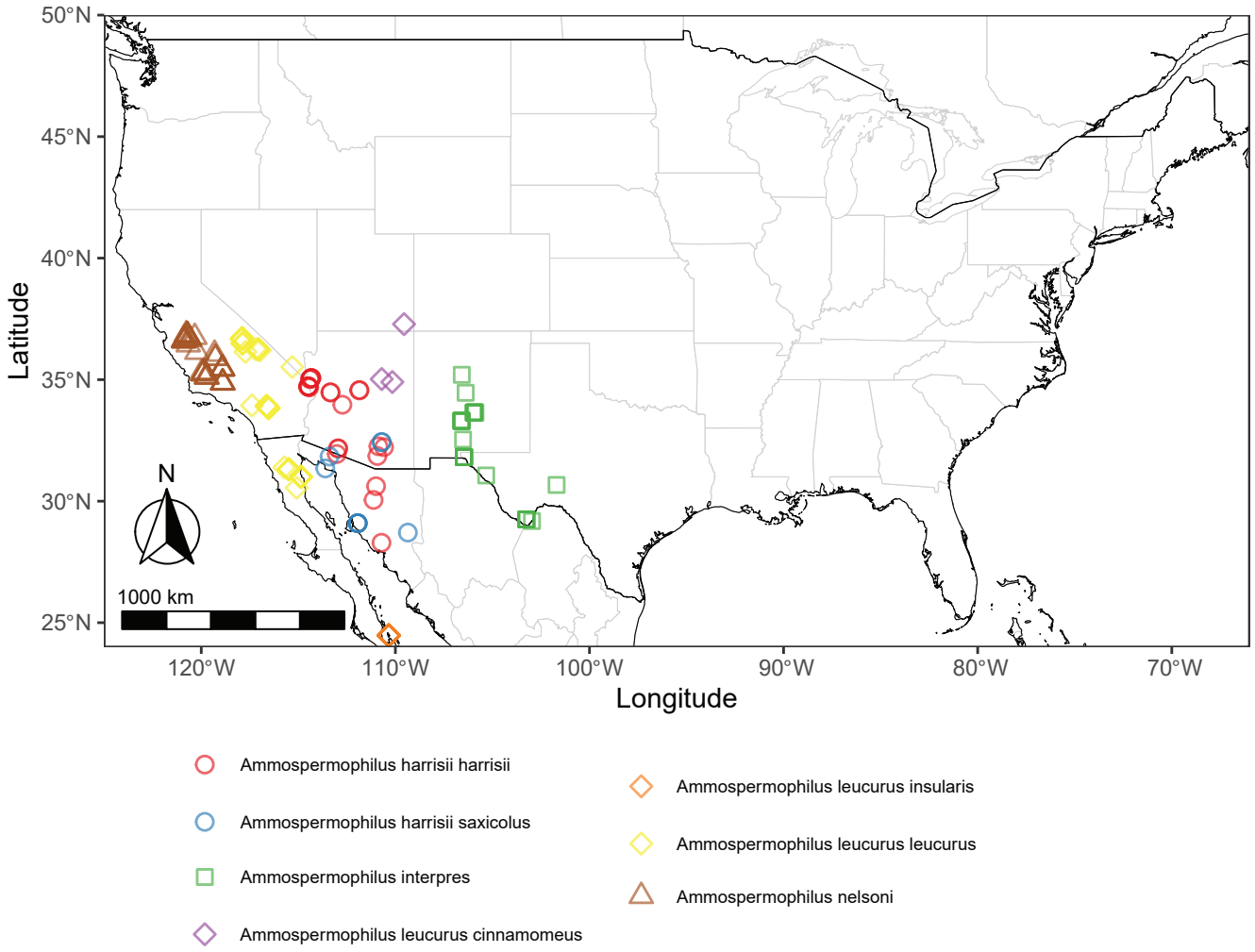

Fig. S1. Zoomed-out locality map of sampled specimens with species shown by symbols and subspecies by colors. Geographic coordinates are in Data S1. Map generated using ggplot2 and rnaturalearth.

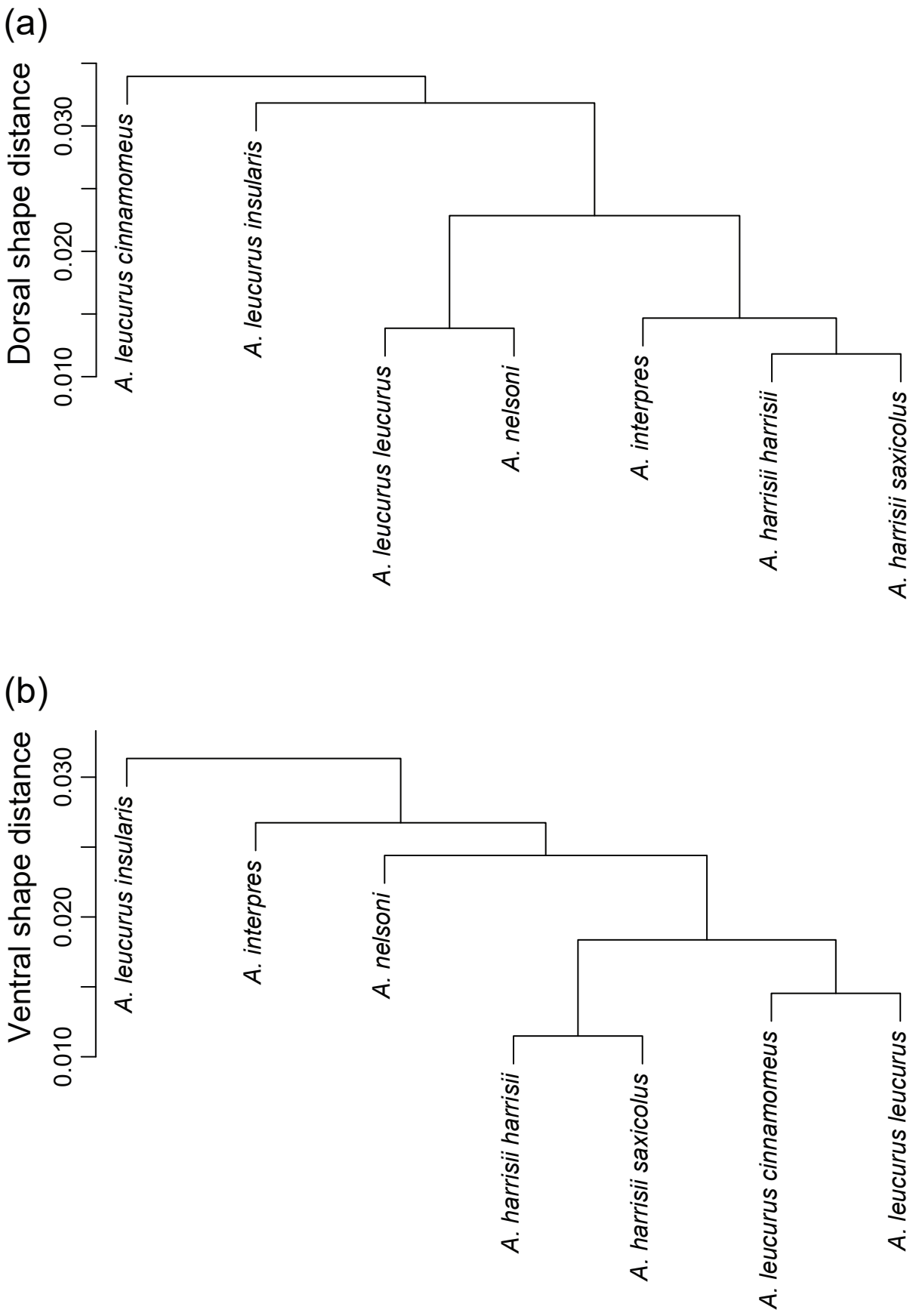

Fig. S2. UPGMA dendrograms based on (a) dorsal and (b) ventral subspecies-mean Procrustes distance matrices. Plots generated using base R package.